

## Neutron diffraction and NQR study of the intermediate turn angle phase formed during AFI to AFII reordering in $\text{YBa}_2\text{Cu}_{3-x}\text{Al}_x\text{O}_{6+\delta}$

E. Brecht,\* W. W. Schmahl,† and H. Fuess

*Fachbereich Materialwissenschaft, Fachgebiet Strukturforchung, Technische Hochschule Darmstadt, Petersenstrasse 23, D-64287 Darmstadt, Germany*

S. Schmenn and H. Lütgemeier‡

*Forschungsanlage Jülich, Institut für Festkörperforschung 4, P.O. Box 1913, D-52425 Jülich, Germany*

N. H. Andersen and B. Lebech

*Risø National Laboratory, Department of Solid State Physics, P.O. Box 49, DK-4000 Roskilde, Denmark*

Th. Wolf

*Forschungszentrum Karlsruhe, Institut für Technische Physik, P.O. Box 3640, D-76021 Karlsruhe, Germany*

(Received 16 December 1996; revised manuscript received 5 March 1997)

The reordering mechanism from the antiferromagnetic phase AFI to the antiferromagnetic phase AFII in an oxygen-deficient  $\text{YBa}_2\text{Cu}_{2.94}\text{Al}_{0.06}\text{O}_{6+\delta}$  single crystal with an oxygen content  $\delta=0.18$  in the Cu(1) layer has been studied by neutron diffraction and nuclear quadrupole resonance (NQR). The crystal orders magnetically from the paramagnetic state to the antiferromagnetic AFI state at the Néel temperature  $T_N=403$  K with an empirical critical exponent of  $\beta=0.26$ . Reordering to the antiferromagnetic AFII state sets in at  $T_2=12$  K. In both the AFI and AFII phases the ordered magnetic moments on the Cu(2) lattice sites are identical and take a value of  $\langle S \rangle_{\text{Cu}(2)} \approx 0.56\mu_B$ ; no ordered moment is found on the Cu(1) lattice sites. From the temperature dependence of the Cu(1) NQR spectrum, the magnetic hyperfine field at Cu(1) sites is found to vary continuously as a function of temperature. This result indicates unequivocally that the AFI $\leftrightarrow$ AFII reordering takes place via a noncollinear intermediate turn angle phase AFI $\oplus$ II. [S0163-1829(97)00826-6]

### I. INTRODUCTION

It is well established that  $\text{YBa}_2\text{Cu}_3\text{O}_{6+\delta}$  exhibits a transition from the metallic and superconducting phase to an insulating and antiferromagnetically ordered phase, when the oxygen content  $\delta$  within the Cu(1) layer is kept below 0.4.<sup>1-4</sup> The antiferromagnetic structure AFI was solved by Tranquada *et al.*<sup>1</sup> in polycrystalline samples using magnetic neutron diffraction. In this phase the spins on the Cu(2) sites alternate antiferromagnetically within the  $\text{CuO}_2$  planes and along the tetragonal  $c$  axis. The average ordered moment on the Cu(2) lattice site was found to be about  $0.52\mu_B$  with the spins oriented perpendicular to the  $c$  axis.<sup>5,6</sup> In contrast no ordered magnetic moment was found on the Cu(1) sites in the oxygen-deficient layer. Taking into account the coupling parameters  $J$  determined by inelastic neutron scattering techniques<sup>6-8</sup> the AFI phase can be characterized by antiferromagnetic bilayers formed by the moments on nearest-neighbor Cu(2) layers, which are weakly antiferromagnetically coupled along the tetragonal  $c$  axis.

Magnetic neutron-diffraction studies were reported for reduced polycrystalline material as well as for undoped  $\text{YBa}_2\text{Cu}_3\text{O}_{6+\delta}$  single crystals, which all show the AFI phase with approximately the same values for  $T_N$  and for the average ordered magnetic moment for a given oxygen content.<sup>2-5,9,10</sup> However, Kadowaki *et al.*<sup>11</sup> and later Shamoto *et al.*<sup>6</sup> reported a reordering to a second antiferromagnetic phase AFII at low temperature with a transition tem-

perature  $T_2$  of about 40 K and 15 K for apparently undoped  $\text{YBa}_2\text{Cu}_3\text{O}_{6+\delta}$  single crystals, respectively. This antiferromagnetic low-temperature phase has a similar antiferromagnetic arrangement of the spins within the Cu(2) layer as the AFI phase, but a different stacking of the spins along the  $c$  axis, which results in a doubling of the magnetic unit cell along  $c$ .<sup>11</sup> The moments on Cu(2) sites in the AFII phase can also be described by antiferromagnetic bilayers that experience a coupling along the  $c$  axis which is ferromagnetic in nature.

It is well known that the physical as well as the structural properties are strongly affected in  $\text{YBa}_2\text{Cu}_{3-x}\text{M}_x\text{O}_{6+\delta}$  doped with trivalent ions  $\text{M}^{3+}=\text{Al}^{3+}, \text{Co}^{3+}, \text{Fe}^{3+}$  on the Cu(1) sites.<sup>12-24</sup> Magnetic neutron-scattering investigations on Co-doped<sup>25-27</sup> and Fe-doped<sup>28-32</sup> ceramic samples and our own recent studies on Al-doped single crystals<sup>33,34</sup> show that the AFII phase can be stabilized by the doping of trivalent defect ions. At low doping levels the  $\text{Co}^{3+}, \text{Fe}^{3+}$ , and  $\text{Al}^{3+}$  defects show a similar influence on the magnetic properties and force the reordering from the AFI to the AFII phase at low temperatures. However, for high substitution levels the Co- and Fe-doped systems differ from the Al-doped system, which may result from the magnetic character of the dopants. In the Al-doped system with  $x<0.2$  the reordering temperature to the AFII phase,  $T_2$ , was always observed to be lower than 20 K.<sup>34</sup> In contrast, the AFII phase is stabilized in the Co- and Fe-doped systems for high substitution levels over the whole antiferromagnetic regime.

TABLE I. Results of the structural refinement of the neutron Bragg data set ( $T=298$  K). The Debye-Waller factor has the form  $\exp[-2\pi^2[a^{*2}(h^2U_{11}+k^2U_{22})+l^2c^{*2}U_{33}]]$ , where the  $U_{ii}$  are the mean-square displacements.

Atom	Position	$x/a$	$y/b$	$z/c$	$K$	$U_{11}$	$U_{22}$	$U_{33}$
Y	1d	0.5	0.5	0.5	1	0.0043(7)	$=U_{11}$	0.0079(11)
Ba	2h	0.5	0.5	0.19525(20)	2	0.0084(8)	$=U_{11}$	0.0053(12)
Cu(1)	1a	0	0	0	0.94(3)	0.0162(11)	$=U_{11}$	0.0084(14)
Al	1a	0	0	0	0.06(3)	0.0162(11)	$=U_{11}$	0.0084(14)
Cu(2)	2g	0	0	0.36056(14)	2.01(2)	0.0037(5)	$=U_{11}$	0.0096(8)
O(1)	2g	0	0	0.15270(23)	1.94(4)	0.0180(10)	$=U_{11}$	0.0132(14)
O(2)	4i	0.5	0	0.37856(15)	4.08(6)	0.0051(7)	0.0078(7)	0.0121(8)
O(4)	2f	0	0.5	0	0.18(3)	0.115(51)	0.026(22)	0.023(22)
Lattice parameters (293 K)				$a=3.863(3)$ Å	$c=11.779(9)$ Å			
Residuals				$R=0.032$	$R_w=0.027$			

The antiferromagnetic ordering has been intensively studied also by Cu nuclear quadrupole resonance (NQR) experiments.<sup>35–45</sup> It was verified by NQR that only the moments on the Cu(2) sites exhibit the antiferromagnetic ordering and that the Cu(2) moments are oriented perpendicular to the  $c$  axis.<sup>35–38</sup> The presence of the AFII phase in Fe-doped materials was reported by Lütgemeier.<sup>39</sup> The reordering temperature  $T_2$  from the AFI phase to the AFII phase depends strongly on the Fe content  $x$  of the samples<sup>40,41</sup> as well as on the oxygen content  $\delta$  within the Cu(1) layer.<sup>42</sup> In particular increasing the oxygen content  $\delta$  leads to a depression of the AFII phase.<sup>42</sup> Therefore it has been suggested that the reordering from the AFI phase to the AFII phase cannot be triggered by threefold-coordinated  $\text{Cu}^{2+}$  ions within the Cu(1) layer,<sup>41,43</sup> which was postulated by Kadowaki and co-workers.<sup>11</sup> The nature of the AFI $\leftrightarrow$ AFII reordering has been attributed to the magnetic moment of the  $\text{Fe}^{3+}$  defect ions within the Cu(1) layer,<sup>42,43</sup> which leads to a frustration with respect to the moments on neighboring Cu(2) sites. However, this explanation is only part of the truth, since it has been found that  $\text{Al}^{3+}$  and  $\text{Ga}^{3+}$ , which are definitely nonmagnetic, also lead to a Zeeman splitting of the Cu(1) NQR line at low temperature.<sup>44,45</sup>

In order to improve our understanding of the mechanisms leading to the transition from the AFI to the AFII phase it is essential to establish whether it takes place via a first-order transition with defect-induced phase coexistence or continuously via two possibly second-order transitions with an intermediate spin-canting phase. Since we concluded in our previous study<sup>34</sup> that this problem could not be solved by neutron diffraction alone, we have investigated an  $\text{YBa}_2\text{Cu}_{2.94}\text{Al}_{0.06}\text{O}_{6.18}$  single crystal by neutron diffraction as well as by NQR.

## II. EXPERIMENT

Al-doped single crystals were grown in air from a BaO/CuO flux in an  $\text{Al}_2\text{O}_3$  crucible by the slow-cooling method<sup>46</sup> at a cooling rate of 0.5 K/h.<sup>34</sup> The crystal was deoxygenated at 923 K under the same conditions as in Ref. 5 using a gas volumetric technique.<sup>47</sup> Under these conditions Casalta *et al.*<sup>5</sup> attained an oxygen content of  $\delta=0.1$  for an apparently undoped crystal. The full width at half maximum (FWHM) of the rocking curve of the (005) reflection analyzed by high-

resolution x-ray diffractometry with Cu  $K\alpha_1$  radiation was  $\sim 0.03^\circ$  and purely resolution limited, indicating a small mosaic spread.

Nonpolarized magnetic neutron-diffraction experiments were performed with the instrumentation described in Ref. 34 (TAS1 triple-axis spectrometer at the DR3 reactor at Risø National Laboratory, graphite monochromator, incident neutrons of energy 13.7 meV). The crystal was oriented with the [110] axis vertical, and thus all the scans were performed in the ( $hhl$ ) scattering plane. The single crystal had a platelike shape with a size of about  $3 \times 4 \times 0.5$  mm<sup>3</sup>.

In order to characterize the single crystal structurally and to determine the Al and O contents, a complete nuclear Bragg scattering set was collected as described in Ref. 34 [TAS2 four-circle diffractometer at DR3, incident neutrons  $\lambda=1.047$  Å,  $\theta$ - $2\theta$  data collection, 1052 nuclear Bragg reflections in half-sphere collected up to  $\sin\theta/\lambda=0.67$  Å<sup>-1</sup>, 192 independent observations, structure analysis with SHELX76 (Ref. 48)]. The structural parameters determined from the four-circle data were used in the subsequent analysis of the magnetic data.

The NQR spectra were recorded by a frequency sweep using a standard spin-echo technique with quadrature detection. For measurements between 4.2 K and 17 K the sample was mounted in an Oxford Instruments CF1200 <sup>4</sup>He cryostat.

## III. RESULTS

### A. Nuclear structure

The results of the refinement are shown in Table I and can be summarized as follows: Al is found to occupy exclusively the Cu(1) lattice site. The population factor of Al on Cu(1) was refined to 0.06. Within the experimental error no Al enters Cu(2) lattice sites [the refinement of Al on Cu(2) sites gave a negative population factor for Al on this site]. The apical oxygen is not fully occupied but shows a small deficiency of about 3%. For this Al-doped single crystal with an Al content of  $x=0.06(2)$  an oxygen content  $\delta=0.18(3)$  is obtained on the O(4) sites in the basal plane. Since this single crystal was reduced under the same conditions as the undoped crystal in Ref. 5, the oxygen content found in the basal plane can be directly compared to the undoped system,

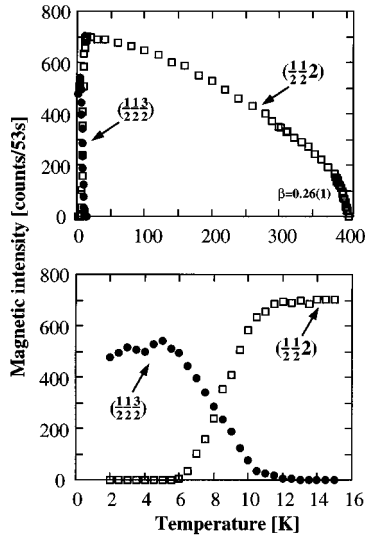


FIG. 1. Integrated intensity vs temperature for the  $(\frac{1}{2}\frac{1}{2}2)$  ( $\square$ ) and  $(\frac{1}{2}\frac{1}{2}\frac{3}{2})$  ( $\bullet$ ) magnetic reflections. The order parameter  $M \propto \sqrt{I}$  shows a power law behavior  $M \propto |T - T_N|^\beta$  with a critical exponent  $\beta = 0.26(1)$  fitted between 300 K and the Néel temperature  $T_N = 403$  K. At low temperatures AFII is the stable phase; between 6 K and 12 K ordering components of both phases coexist.

which gives an oxygen content  $\delta = 0.10$ . The higher oxygen content in the Al-doped crystal is due to the aluminum ions in the Cu(1) layer, which pin a significant amount of residual oxygen.

### B. Neutron diffraction studies of the AFI $\leftrightarrow$ AFII reordering

Figure 1 shows the integrated intensity of the  $(\frac{1}{2}\frac{1}{2}2)$  and  $(\frac{1}{2}\frac{1}{2}\frac{3}{2})$  magnetic Bragg peaks versus temperature, which arise due to the antiferromagnetic ordering components AFI and AFII, respectively. The transition from the paramagnetic phase to the AFI phase was found at  $T_N = 403(1)$  K. The magnetic intensity of the AFI phase can be well described by a power law  $I \propto I_0(T_N - T)^{2\beta}$  with a critical exponent  $\beta = 0.26$  (fitted between 300 K and  $T_N$ ). Reordering to the AFII phase sets in at 12 K. In the limited temperature interval between 6 K and 12 K both the AFI and AFII ordering components coexist. Below 6 K the AFI ordering component vanishes completely. The AFII order parameter exhibits a maximum at about 5 K, and it shows a tendency to decrease with decreasing temperature. Such a reentrant behavior is well known from the undoped system<sup>4,49</sup> and is explained by the building up of static disorder between the antiferromagnetic bilayers at low temperatures, which results from a small amount of localized oxygen  $2p$  holes transferred to the  $\text{CuO}_2$  planes.

The sharpness of the magnetic Bragg peaks indicating three-dimensional long-range order was similar to those of the crystals described in our previous paper.<sup>34</sup> The magnetic moments in the two antiferromagnetic phases were determined from the intensity of 9-11 magnetic peaks at 20 K and 4.2 K. A table of the observed and calculated magnetic structure factors can be obtained from the authors.

The periodicity of long-range order in the AFI phase (Fig. 1 in Ref. 34) is expressed by the wave vector  $\vec{q}_{\text{AFI}} = (\frac{1}{2}\frac{1}{2}0)$  in reduced reciprocal lattice units. Hence the AFI phase gives

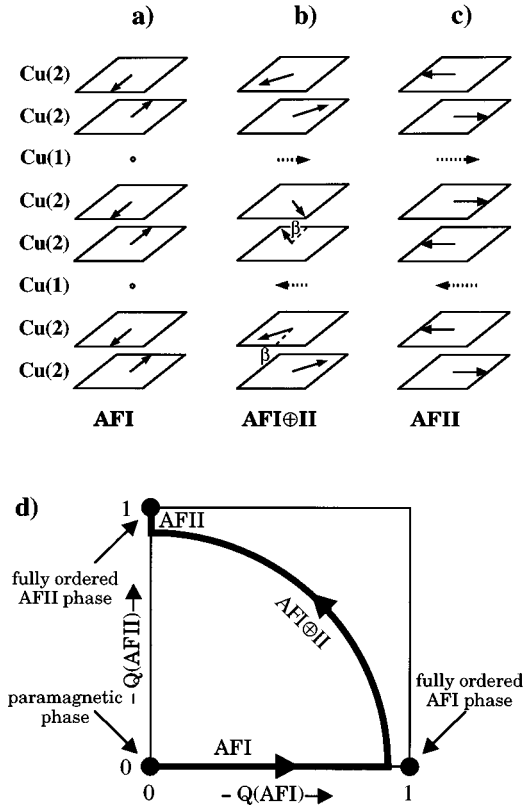


FIG. 2. Top: stacking of the spins along the  $c$  axis in the (a) AFI, (b) the AFII, and (c) the intermediate-turn-angle phase  $\text{AFII} \oplus \text{II}$ . The moments in the collinear AFI are assumed to be perpendicular to the moments in the collinear AFII phase. Note that a defect-induced magnetic moment on the Cu(1) sites will be frustrated in AFI but not in AFII. The resultant spin structure of the noncollinear intermediate phase  $\text{AFII} \oplus \text{II}$  results from a vector summation of the two collinear structures leading to the canting angle  $\beta$ . Bottom: phase-space diagram indicating the evolution of the amplitudes  $Q$  (order parameters) of the AFI and the AFII ordering schemes with decreasing temperature. The turn angle rotates continuously as the amplitude  $Q(\text{AFI})$  is replaced by  $Q(\text{AFII})$ . Note that the hyperfine field at the Cu(1) site is zero for the AFI ordering scheme as the contributions from neighboring spins cancel. For AFII, however, the contributions add to a strong nonzero field. In the turn angle phase, the hyperfine field takes intermediate values. Further note that the spins rotate in the same sense within a  $\text{Cu}(2)\text{O}_2$  double layer, while the sense of rotation alternates across the Cu(1) position from double layer to double layer.

rise to magnetic peaks that can be indexed as  $(h'k'l') = (h + \frac{1}{2}, k + \frac{1}{2}, l)$ , for  $h, k, l$  integer. The moments on Cu(2) sites form antiferromagnetically ordered bilayers. The bilayers are weakly antiferromagnetically coupled along the tetragonal  $c$  axis across the Cu(1) layer (Fig. 1 in Ref. 34). A simplified view of the stacking along  $c$  is shown in Fig. 2(a). For the AFI phase at 20 K we obtained an average ordered moment of the  $\text{Cu}^{2+}$  ions on the Cu(2) sites of  $0.54(2)\mu_B$  ( $R$  value 3.3%, 11 magnetic reflections); the ordered moment on Cu(1) sites is zero for symmetry reasons.

The periodicity of the AFII long-range order is characterized by the wave vector  $\vec{q}_{\text{AFII}} = (\frac{1}{2}\frac{1}{2}\frac{1}{2})$  leading to magnetic peaks which can be indexed as  $(h'k'l') = (h + \frac{1}{2}, k + \frac{1}{2}, l + \frac{1}{2})$ , for  $h, k, l$  integer. Similar to the AFI phase the mo-

ments on Cu(2) sites form antiferromagnetically ordered bilayers with an ordered moment of  $0.56(1)\mu_B$  on Cu(2) sites at 4.2 K ( $R$  value 3.0%, 9 magnetic reflections), as schematically shown in Fig. 2(c). The *ordered* moment on Cu(1) sites was refined to  $-0.001(5)\mu_B$ . This means that there is no *ordered* magnetic moment on the Cu(1) chain sites in the AFII phase, in agreement with NQR measurements that also exclude any ordered magnetic moment at the Cu(1) site with the upper limit of  $0.03\mu_B$ .<sup>43</sup>

The value of the *ordered* moment  $\langle S \rangle_{\text{Cu}(2)}$  in the AFII phase is in good agreement with recent studies<sup>34</sup> on a  $\text{YBa}_2\text{Cu}_{3-x}\text{Al}_x\text{O}_{6+\delta}$  single crystal with  $x=0.19$  and  $\delta=0.28$ , where  $\langle S \rangle_{\text{Cu}(2)}$  was found to be  $0.55(1)\mu_B$ . This implies that the value of the magnetic moment in the AFII phase does not seem to be related to the Al content  $x$ . It is noteworthy that the comparison of the magnetic properties of these two single crystals is absolutely justified, although their oxygen content is different. Since the Néel temperature  $T_N$  of 407 K in  $\text{YBa}_2\text{Cu}_{2.81}\text{Al}_{0.19}\text{O}_{6.28}$  is almost equal to the  $T_N$  of 403 K observed here, the higher amount of oxygen  $\delta$  in  $\text{YBa}_2\text{Cu}_{2.81}\text{Al}_{0.19}\text{O}_{6.28}$  arises purely from the higher Al content of this sample due to the tetrahedral coordination of  $\text{Al}^{3+}$  and these excess oxygen ions do not contribute to the transfer of charge to the Cu(2) layer.

### C. NQR studies of the AFI $\leftrightarrow$ AFII reordering

NQR spectroscopy is an excellent tool to probe the magnetic configuration on a local scale. Thus this technique gives important complementary information to neutron Bragg diffraction that exclusively reflects the long-range correlated average spin structure.

Natural copper consists of the two isotopes  $^{63}\text{Cu}$  and  $^{65}\text{Cu}$  with the natural abundance of 69% and 31%, respectively. Both isotopes show a nuclear spin  $I$  of  $\frac{3}{2}$ . The quadrupole moment couples to the electric field gradient (EFG) resulting from the charge distribution around the atomic site. The EFG is a traceless second-rank tensor and can be expressed by the largest eigenvalue  $V_{zz}$  and by the asymmetry parameter  $\eta$ . In the case of an EFG without external magnetic field, the degeneracy of the  $\pm m$  levels is retained and for Cu with  $I=\frac{3}{2}$  only one NQR line at the frequency  $\nu_{\text{NQR}} = \nu_q \sqrt{1 - \eta^2/3}$  with the quadrupole frequency  $\nu_q = eQV_{zz}/2h$  can be observed. In the case of an existing external or internal magnetic field, the degeneracy of the  $\pm m$  levels is broken and a Zeeman splitting of the NQR line occurs.

In the following, all frequencies are related to the isotope  $^{63}\text{Cu}$  and the corresponding frequencies of the isotope  $^{65}\text{Cu}$  are roughly 10% smaller. In antiferromagnetic  $\text{YBa}_2\text{Cu}_3\text{O}_6$  (AFI) the NQR line of the Cu(1) site can be observed at the NQR frequency of 30.1 MHz.<sup>40</sup> The spectrum for this 30.1 MHz line of the Cu(1) site in the pure system reveals single lines without any magnetic splitting.<sup>35,39</sup> From the antiferromagnetic NMR spectrum of  $\text{YBa}_2\text{Cu}_3\text{O}_6$  a hyperfine field of 7.965 T at the Cu(2) site can be deduced.<sup>36</sup> The fact that no Zeeman splitting of the Cu(1) NQR line can be observed in the AFI structure implies that the dipolar and magnetic hyperfine fields from the moments on the Cu(2) sites cancel exactly at the Cu(1) sites. This situation is shown in Fig. 2, where the next-nearest-neighboring moments on Cu(2) sites

are antiferromagnetically coupled along the  $c$  axis. In contrast, however, the  $\text{Cu}(2)\cdots\text{Cu}(2)$  coupling along the  $c$  axis in the AFII structure is ferromagnetic (Fig. 2), and the magnetic Cu(2) ions induce a dipolar and magnetic hyperfine field at the Cu(1) site, which leads to a splitting of the Cu(1) NQR line. This has been shown by Lütgemeier and Rupp<sup>39,40</sup> in the Fe-doped system at low temperature, who observed a well-resolved splitting of the NQR lines by a magnetic field of about 170 mT.

The NQR spectra of our  $\text{YBa}_2\text{Cu}_{2.94}\text{Al}_{0.06}\text{O}_{6.18}$  single crystal are shown in Fig. 3. By careful analysis and line profile fitting we were able to resolve the spectra in Fig. 3. Zeeman splitting sets in below 11 K and reaches its full value of 198 mT at 5 K. The spectra rule out a simple coexistence of pure AFI and AFII states of varying population with temperature. It is evident from Fig. 3 that continuous spectral changes of the Zeeman splitting occur through intermediate values of the hyperfine field. If there are any discontinuities, they occur between AFI and the intermediated states, rather than between AFI and AFII. Unfortunately the spread of values of local hyperfine fields indicates that the crystal is inhomogeneous with respect to its magnetic properties.

It is important to note that in the case of Fe doping, a similar linear increase with decreasing temperature has been found.<sup>43</sup> However, at a comparable doping level ( $x_{\text{Fe}}=0.048$ ,  $x_{\text{Al}}=0.06$  for the crystal investigated here), the transition starts at a much higher temperature  $T_2$  of 140 K. By careful analysis and line profile fitting we were able to resolve the spectra in Fig. 3 into two to three components with different values of the local field and relative intensity [Figs. 4(a) and 4(b)]. For example at 8 K, only 25% of the Cu(1) sites experience the full local field (198 mT) of the AFII configuration and 19% of the sites experience no field at all; the remaining 56% of the sites experience a reduced field of the order of 122 mT. It should be noted, however, that the two to three components may be a crude representation of a more continuous distribution of hyperfine fields. To distinguish between a continuous second-order transition mechanism or a first-order transition with defect-induced phase coexistence it is important to address the question of hysteresis. Neither the neutron-diffraction studies of Kawasaki *et al.*<sup>11</sup> on an apparently undoped crystal nor our own neutron-diffraction studies on Al-doped single crystals<sup>34</sup> gave any indication for a hysteresis at the AFI-AFII transition. Probing the local magnetic configurations by NQR, which is more appropriate to analyze defect-related effects, we did not find any hysteresis either. Figures 5(a) and 5(b) show the cooling-down and heating-up NQR spectra at 7 K. Within the experimental error the spectra are identical with a Zeeman splitting of about 158 mT.

## IV. DISCUSSION

Our neutron-diffraction studies as well as the temperature-dependent NQR studies on an  $\text{YBa}_2\text{Cu}_{2.94}\text{Al}_{0.06}\text{O}_{6.18}$  crystal show that the AFI $\leftrightarrow$ AFII reordering takes place within a limited temperature interval. While above about 12 K the pure AFI phase exists, below about 5 K the pure AFII phase is present. A possible origin of the AFI $\leftrightarrow$ AFII transition was suggested in our previous

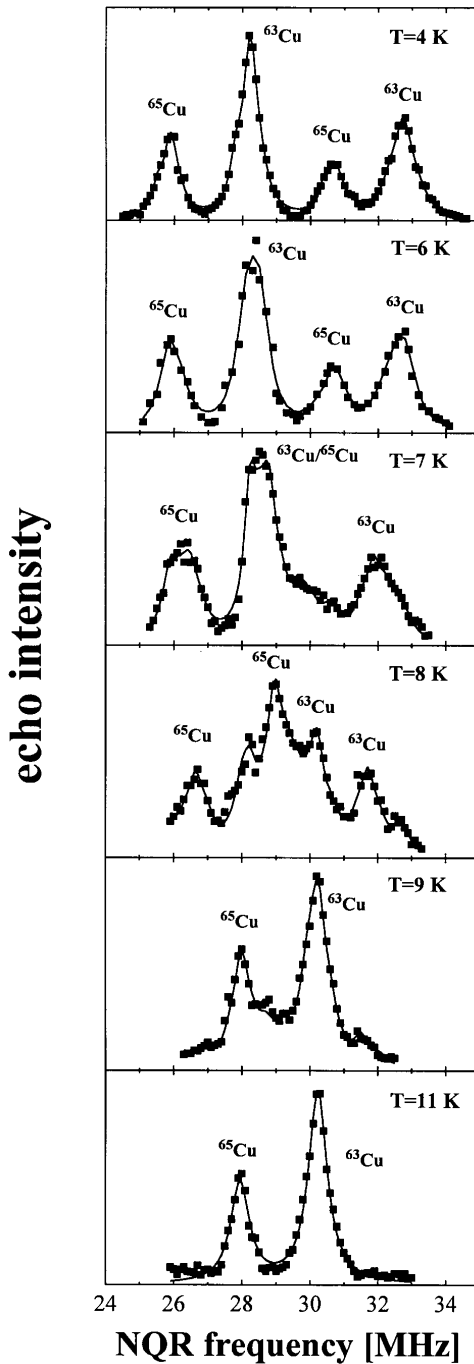


FIG. 3. Cu(1) NQR line as a function of temperature. At 4.2 K the NQR line shows a Zeeman splitting; the hyperfine field takes a value of 198 mT, indicating the presence of the AFII phase. Increasing the temperature results in a decrease of the Zeeman splitting.

paper<sup>34</sup> on the magnetic structure of Al-doped single crystals. From structural-chemical principles we concluded that the Al-doping and  $\text{Al}^{3+}$ -defect distributions may have significant influence on the AFI  $\leftrightarrow$  AFII reordering. In particular, a random Al distribution will give rise to  $\text{Al}^{3+}\text{-O}^{2-}\text{-Cu}^{2+}$  fragments with free  $\text{Cu}^{2+}$  spins within the Cu(1) layer. If these moments on the Cu(1) sites couple magnetically to the Cu(2)O<sub>2</sub> layer, there will be frustration of the antiferromagnetic arrangement of the moments on the neighboring Cu(2) sites which may be resolved in the AFII phase. That this is

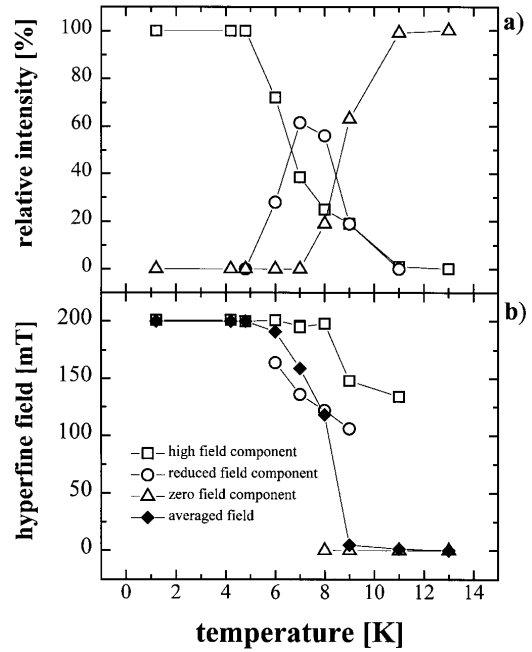


FIG. 4. Relative intensity (a) and hyperfine field (b) at different temperatures, determined by fitting the NQR spectra in Fig. 3 with up to three contributing components.

indeed the case has recently been established by Andersen and Uimin<sup>50</sup> who show that polarization of free spins in the Cu(1) layer mediates an effective ferromagnetic coupling between adjacent Cu(2)O<sub>2</sub> bilayers at low temperatures.

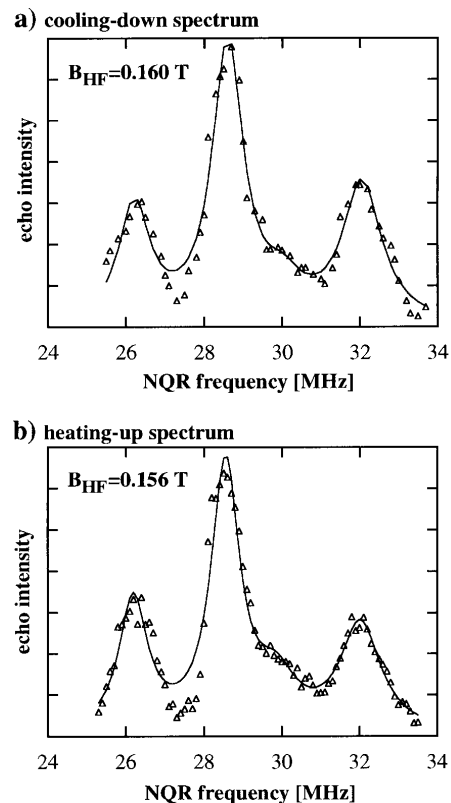


FIG. 5. Warming-up (a) and cooling-down (b) Cu(1) NQR spectra at 7 K. Within the experimental error the hyperfine field at Cu(1) takes the same value of 0.155 T.

For the characterization of the nature of the transition from the AFI phase to the AFII phase two different possibilities must be taken into account: The reordering between the AFI phase and the AFII phase can take place either via a direct, strictly first-order transition with phase coexistence or in a more or less continuous way by two possibly second-order transitions via an intermediate phase  $\text{AFI} \oplus \text{II}$ . The symmetry of the intermediate phase is the common subgroup of AFI and AFII, and the structure may be envisaged as a vectorial superposition of AFI and AFII components. This superposition leads to a canted spin structure, where the canting angle is able to rotate continuously between the AFI and the AFII configuration [cf. Fig. 2(b)].

Kadowaki *et al.*<sup>11</sup> developed a simple model calculation for the energy of the spin system within the molecular-field approximation. A very similar but more extensive calculation has recently been published by Mirebeau and co-workers.<sup>30</sup> However, both these models rely on the presence of an *ordered* magnetic moment in the Cu(1) layer, which is not observed experimentally, and they cannot account for the temperature dependence of the transition from the AFII to the AFI phases. A more comprehensive account is given by Andersen and Uimin.<sup>50</sup> These authors show that the effective ferromagnetic coupling between the  $\text{Cu}(2)\text{O}_2$  bilayers, which is mediated by polarization of free spins in the Cu(1) layers, stabilizes the AFII phase at low temperatures, and in agreement with the present experimental results, their model predicts that the  $\text{AFI} \leftrightarrow \text{AFII}$  reordering takes place via a distinct intermediate turn angle phase  $\text{AFI} \oplus \text{II}$ .

As previously mentioned<sup>34</sup> neutron diffraction is not able to discriminate between either a  $\text{AFI}$ - $\text{AFII}$  phase coexistence in different parts of an inhomogeneous crystal on the one hand or the turn angle phase on the other hand. This problem will be briefly discussed in the following. In the case of a direct first-order transition from the AFI phase [cf. Fig. 2(a)] and the AFII phase [cf. Fig. 2(b)] the coexistence of magnetic Bragg peaks of the AFI and AFII phase must be attributed to inhomogeneities in the sample. Therefore the ratio between the intensities  $I_{\text{AFI}}(T)$  and  $I_{\text{AFII}}(T)$  at a certain temperature  $T$  is directly proportional to the ratio of the volumina  $V_{\text{AFI}}(T)$  and  $V_{\text{AFII}}(T)$  and can be simply expressed by

$$\frac{I_{\text{AFII}}(T)}{I_{\text{AFI}}(T)} = \frac{V_{\text{AFII}}(T)}{V_{\text{AFI}}(T)} \frac{|\vec{F}_{\text{AFII}}|^2}{|\vec{F}_{\text{AFI}}|^2} \propto \frac{V_{\text{AFII}}(T)}{V_{\text{AFI}}(T)}. \quad (4.1)$$

The constant  $|\vec{F}_{\text{AFI}}|^2$  corresponds to the square of the structure factor of a magnetic AFI peak at a temperature, where the peaks of the AFII phase completely vanish (e.g., 20 K in Fig. 1), and accordingly  $|\vec{F}_{\text{AFII}}|^2$  to the square of the structure factor of a magnetic AFII peak at a temperature, where the peaks of the AFI phase completely vanish (e.g., 5 K in Fig. 1).

In the case of an intermediate turn-angle phase, the structure factor of the noncollinear intermediate phase can be interpreted as the vectorial superposition of the structure factors of the AFI and AFII phases. Therefore this noncollinear structure results in magnetic peaks with integer as well as with half-integer  $l'$ . The geometrical part of the structure factor of the intermediate phase shown in Fig. 2(b) takes the form

$$|\vec{F}_{\text{geo}}^{\text{AFI} \oplus \text{II}}(\vec{\kappa})| \propto \begin{cases} 2\langle S \rangle_{\text{Cu}(2)} \cos\beta \sin(2\pi l'_I z) & \text{for } l'_I = \text{integer,} \\ 2\langle S \rangle_{\text{Cu}(2)} \sin\beta \cos(2\pi l'_{\text{II}} z) & \text{for } l'_{\text{II}} = \text{half-integer,} \end{cases} \quad (4.2)$$

where  $\vec{\kappa}$  is the scattering vector,  $\langle S \rangle_{\text{Cu}(2)}$  is the thermal average of the ordered moment on Cu(2) sites, and  $z$  the distance between the Cu(1) and Cu(2) layers as a fraction of the unit cell length  $c$ .  $\beta$  describes the canting angle as defined in Fig. 2(b). The ratio of the square of the magnetic structure factors with integer  $l'_I$  and half-integer  $l'_{\text{II}}$ , which we will name for simplicity  $|\vec{F}_{\text{AFI}}(T)|^2$  and  $|\vec{F}_{\text{AFII}}(T)|^2$ , at a certain temperature  $T$  can be written as

$$\begin{aligned} \frac{|\vec{F}_{\text{AFII}}(T)|^2}{|\vec{F}_{\text{AFI}}(T)|^2} &= \tan^2\beta(T) \left( \frac{\cos(2\pi l'_{\text{II}} z)}{\sin(2\pi l'_I z)} \right)^2 \\ &\times \left( \frac{f^2(\vec{\kappa}^{\text{II}})}{f^2(\vec{\kappa}^{\text{I}})} \right)^2 \frac{\langle 1 - (\hat{\kappa}^{\text{II}} \cdot \hat{S})^2 \rangle}{\langle 1 - (\hat{\kappa}^{\text{I}} \cdot \hat{S})^2 \rangle} \\ &\propto \tan^2\beta(T). \end{aligned} \quad (4.3)$$

$f(\vec{\kappa})$  is the magnetic form factor for  $\text{Cu}^{2+}$ , for which we used an aspherical expression calculated for a  $3d_{x^2-y^2}$  electron distribution.<sup>6</sup> Equations (4.1) and (4.3) demonstrate that the ratio of  $|\vec{F}_{\text{AFI}}(T)|^2$  and  $|\vec{F}_{\text{AFII}}(T)|^2$  of any pair of magnetic peaks with integer and half-integer  $l'$  can be expressed either by a ratio of the volumina of the AFI and AFII phases, which may vary continuously as a function of temperature, or by a function of a canting angle  $\beta$ , which also varies with  $T$ . Therefore, from the magnetic structure factors, no information can be extracted about the question, if the temperature interval, in which the reordering takes place, corresponds to a mixed phase region or arises from a noncollinear structure. It should be noted that the ratio of the magnetic structure factors for both types of magnetic behavior is always constant; i.e., the ratio between the structure factors remains unaffected in the transition region.

Our NQR investigations, however, demonstrate that the hyperfine field at the Cu(1) site changes with temperature. This hyperfine field  $B_{\text{HF}}$  at the Cu(1) site which results from the moments within the Cu(2) layer is indicated in Figs. 2(a)–2(c). In the case of the AFI phase [Fig. 2(a)], the anti-ferromagnetic arrangement of the moments on neighboring Cu(2) sites cancels at the Cu(1) site, so that no resulting hyperfine field exists there. In the case of the AFII phase [Fig. 2(c)] the moments on neighboring Cu(2) sites are anti-ferromagnetically arranged, leading to a hyperfine field of about 198 mT at the Cu(1) sites.<sup>40</sup> For the noncollinear structure shown in Fig. 2(b) the canted moments on Cu(2) sites result in a *temperature-dependent* hyperfine field  $B_{\text{HF}}(T)$  which is smaller than in the case of the collinear AFII structure. Therefore the canting angle  $\beta$  can be directly related to the hyperfine field  $B_{\text{HF}}$  at the Cu(1) site and takes the form

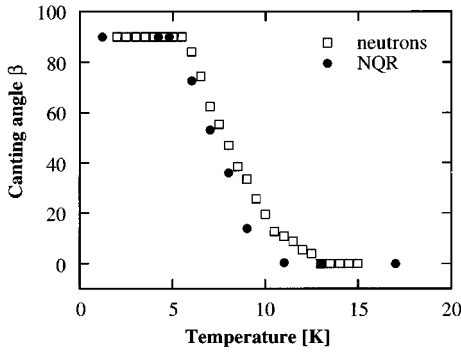


FIG. 6. Comparison between the canting angle deduced from neutron-diffraction studies and the averaged canting angle from the NQR studies.

$$\beta = \arcsin \frac{B_{\text{HF}}(T)}{B_{\text{HF}}(0)}. \quad (4.4)$$

$B_{\text{HF}}(0)$  expresses the hyperfine field at the Cu(1) sites in the pure AFII phase. The canting angle  $\beta$  takes the value  $\beta = 90^\circ$  (AFII phase) for  $B_{\text{HF}}(T) = B_{\text{HF}}(0)$ , and is equal to 0 for  $B_{\text{HF}}(T) = 0$  (AFI phase). Thus, by the temperature dependence of the hyperfine field at the Cu(1) site the NQR experiment is able to demonstrate experimentally the existence of an intermediate phase and therefore directly clarifies the question about the nature of the transition. For a pure first-order phase coexistence the observations would be completely different: The intensity ratio between the AFI and AFII NQR signals would vary while the hyperfine fields of 0 mT for the AFI signal and 198 mT for the AFII signal would remain constant.

Figure 2(d) indicates our interpretation of the transition mechanism in order parameter vector space. Ordering with AFI periodicity [ $\vec{q}_{\text{AFI}} = (\frac{1}{2}\frac{1}{2}0)$ ] has a higher  $T_n$  than potential ordering with AFII periodicity [ $\vec{q}_{\text{AFII}} = (\frac{1}{2}\frac{1}{2}\frac{1}{2})$ ] and sets in first with decreasing temperature. However, AFII ordering gains more internal energy and it is thus the stable phase at low temperature. In the intermediate regime a crossover takes place: The increasing AFII component depresses the AFI component continuously across the stability range of an intermediate turn angle phase AFI $\oplus$ II, where both order parameters are nonzero and superimposed. The vectorial superposition of the two orthogonal order parameters leads to spin canting and a continuous rotation of the spin direction. Such a mechanism has been formulated in terms of Landau theory of order-parameter coupling at a structural phase transition, e.g., by Schmahl.<sup>51</sup>

Figure 6 shows the canting angle deduced from magnetic structure factors according to Eq. (4.3) and from the magnetic hyperfine field according to Eq. (4.4). Although the same crystal has been used for both experiments, the canting angles determined from the NQR experiment seem to be shifted systematically to lower temperatures compared to the diffraction result. Besides a possible systematic error in temperature calibration it is clear that both methods will give different values for the canting angle, if the crystal is inhomogeneous with respect to the magnetic properties. The NQR data indicate such an inhomogeneity (Fig. 3). Further, the decay of the  $(\frac{1}{2}\frac{1}{2}\frac{3}{2})$  magnetic diffraction peak with in-

creasing temperature shows a different slope in the regions between 6 K and 10.5 K and between 10.5 and 12 K which may be related to inhomogeneities. The superimposed spectra of more than one Cu(1) NQR line with different Zeeman splitting have to be interpreted as due to regions with different transition temperatures  $T_2$  and possibly different transition widths. Therefore, apart from the intermediate turn angle phase, the crystal shows regions with AFI and AFII phases [Fig. 4(a)]. These inhomogeneities may arise from a locally different O content within the Cu(1) layer, or more likely from a slightly inhomogeneous distribution of the Al<sup>3+</sup> defect ions. The latter possibility can be directly related to the occurrence of Al clusters during reduction at high temperatures.<sup>24</sup> In summary, within certain limits the NQR experiment allows in principle a separation of these inhomogeneous regions, while the neutron-diffraction experiment averages over the inhomogeneous regions. Therefore the canting angles deduced from the magnetic structure factors are less well suited to describe the variation of the canting angle  $\beta(T)$  as a function of temperature. In contrast, the canting angles  $\beta(T)$  deduced from the NQR experiment are related to the *local* magnetic hyperfine field at a certain region of the crystal. Consequently, the variation of the hyperfine field directly reflects the variation of the canting angle of this particular region.

## V. CONCLUDING SUMMARY

We studied the reordering from the high-temperature AFI phase to the low-temperature AFII phase of a YBa<sub>2</sub>Cu<sub>2.94</sub>Al<sub>0.06</sub>O<sub>6.18</sub> single crystal by neutron-diffraction as well as by the NQR experiments. The reordering takes place via an intermediate turn angle phase. From the neutron-diffraction experiments the structures of the three phases were characterized. It has been found that the averaged magnetic moment on the Cu(2) sites is about  $0.55\mu_B$  in all phases, and no *ordered* magnetic moment is present on the Cu(1) sites. The spin direction is oriented within the (001) plane. From the paramagnetic state the system orders into the antiferromagnetic AFI state at  $T_N = 403$  K. The periodicity of the collinear antiferromagnetic long-range order AFI phase is characterized by the wave vector  $\vec{q}_{\text{AFI}} = (\frac{1}{2}\frac{1}{2}0)$ . The periodicity of the collinear magnetic ordering scheme in the ground state, AFII, is characterized by  $\vec{q}_{\text{AFII}} = (\frac{1}{2}\frac{1}{2}\frac{1}{2})$ . The reordering between AFI and AFII takes place in a limited temperature range between 12 K and about 6 K. Within this temperature range long-range order with both periodicities can be observed by the simultaneous presence of both sets of corresponding magnetic superlattice peaks. The NQR experiment unequivocally demonstrates that this intermediate state is an independent phase with a noncollinear spin structure (rather than AFI/AFII phase coexistence): The observed continuous shifts of the hyperfine field at the Cu(1) site with temperature can be directly related to a continuous change of the spin canting angle in this intermediate phase. Further, the intensity variation of the magnetic neutron Bragg scattering with temperature in the intermediate phase is well described by a spin canting model, if an appropriate vectorial superposition of the competing AFI and AFII spin structures is assumed. The rotation of spin canting is due to a suppression of the AFI ordering amplitude by the growing amplitude of AFII

ordering or vice versa. The large volume fraction of the non-collinear material suggests that this intermediate structure is a true thermodynamically stable phase. By analogy to the linear temperature dependence of the hyperfine-field splitting in the Fe-doped system<sup>43</sup> we conclude that the transition mechanism between the AFI and the AFII phases via an intermediate turn angle phase AFI $\oplus$ II is the same in the Fe- and the Al-doped systems, although the magnetic moment of the Fe<sup>3+</sup> ions leads to a far higher onset temperature  $T_2$ . In summary we have shown that the combination of neutron diffraction and NQR is most suitable to get a more complete picture on the magnetic properties of these compounds.

## ACKNOWLEDGMENTS

The authors would like to thank B. Breiting, J. Lebech, M. Lund, and F. Saxild for their professional technical assistance during the neutron-diffraction experiments. Part of this work was supported by the Danish Ministry of Energy and the CEC Science and Esprit program. The neutron-scattering experiments reported in this paper were performed at the DR3 reactor at Risø National Laboratory and supported by the Commission of the European Community through the Large Installation Plan. E.B. and W.W.S. gratefully acknowledge the Deutsche Forschungsgemeinschaft (DFG) for financial support.

\* Author to whom correspondence should be addressed. Present address: Forschungszentrum Karlsruhe, Institut für Nukleare Festkörperphysik, P.O. Box 3640, D-76021 Karlsruhe, Germany.

† Present address: Allgemeine und Physikalisch-Chemische Mineralogie, Universität Tübingen, Wilhelmstrasse 56, D-72074 Tübingen, Germany.

‡ Passed away on June 11, 1997.

<sup>1</sup>J. M. Tranquada, D. E. Cox, W. J. Kunmann, H. Moudden, M. Suenaga, P. Zolliker, D. Vaknin, S. K. Sinha, M. S. Alvarez, A. J. Jacobson, and D. C. Johnston, *Phys. Rev. Lett.* **60**, 156 (1988).

<sup>2</sup>J. M. Tranquada, A. H. Moudden, A. I. Goldman, P. Zolliker, D. E. Cox, G. Shirane, S. K. Sinha, D. Vaknin, D. C. Johnston, M. S. Alvarez, A. J. Jacobson, J. T. Lewandowski, and J. M. Newsam, *Phys. Rev. B* **38**, 2477 (1988).

<sup>3</sup>P. Burlet, C. Vettier, M. J. G. M. Jurgens, J. Y. Henry, J. Rossat-Mignod, H. Noel, M. Potel, P. Gougeon, and J. C. Levet, *Physica C* **153-155**, 1115 (1988).

<sup>4</sup>J. Rossat-Mignod, P. Burlet, M. J. Jurgens, C. Vettier, L. P. Regnault, J. Y. Henry, C. Ayache, L. Foro, H. Noel, M. Potel, P. Gougeon, and J. C. Levet, *J. Phys. (France) Colloq.* **49**, C8-2119 (1988); J. Rossat-Mignod, L. P. Regnault, C. Vettier, P. Burlet, J. Y. Henry, and G. Lapertot, *Physica B* **169**, 58 (1991); J. Rossat-Mignod, L. P. Regnault, P. Bourges, P. Burlet, C. Vettier, and J. Y. Henry, *ibid.* **192**, 109 (1993).

<sup>5</sup>H. Casalta, P. Schleger, E. Brecht, W. Montfrooij, N. H. Andersen, B. Lebech, W. W. Schmahl, H. Fuess, Ruixing Liang, W. N. Hardy, and Th. Wolf, *Phys. Rev. B* **50**, 9688 (1994).

<sup>6</sup>S. Shamoto, M. Sato, J. M. Tranquada, B. J. Sternlieb, and G. Shirane, *Phys. Rev. B* **48**, 13 817 (1993).

<sup>7</sup>D. Reznik, P. Bourges, H. F. Fong, L. P. Regnault, J. Bossy, C. Vettier, D. L. Milius, I. A. Aksay, and B. Keimer, *Phys. Rev. B* **53**, R14 741 (1996).

<sup>8</sup>S. M. Hayden, G. Aeppli, T. G. Perring, H. A. Mook, and F. Doğan, *Phys. Rev. B* **54**, R6905 (1996).

<sup>9</sup>M. J. Jurgens, P. Burlet, C. Vettier, L. P. Regnault, J. Y. Henry, J. Rossat-Mignod, H. Noel, P. Gougeon, and J. C. Levet, *Physica B* **156-157**, 846 (1989).

<sup>10</sup>D. Petitgrand and G. Collin, *Physica C* **153-155**, 1922 (1988).

<sup>11</sup>H. Kadowaki, M. Nishi, Y. Yamada, H. Takeya, H. Takei, S. M. Shapiro, and G. Shirane, *Phys. Rev. B* **37**, 7932 (1988).

<sup>12</sup>J. M. Tarascon, P. Barboux, P. F. Miceli, L. H. Greene, G. W. Hull, M. Eibschutz, and S. A. Sunshine, *Phys. Rev. B* **37**, 7458 (1988).

<sup>13</sup>T. J. Kistenmacher, *Phys. Rev. B* **38**, 8862 (1988).

<sup>14</sup>B. D. Dunlap, J. D. Jorgensen, C. Segre, A. E. Dwight, J. L.

Matykievicz, H. Lee, W. Peng, and C. W. Kimball, *Physica C* **158**, 397 (1989).

<sup>15</sup>Y. Xu, M. Suenaga, J. Tafto, R. L. Sabatini, and A. R. Modenbaugh, *Phys. Rev. B* **39**, 6667 (1989); Y. Xu, R. L. Sabatini, A. R. Modenbaugh, Y. Zhu, S. G. Shyu, M. Suenaga, K. W. Dennis, and R. W. McCallum, *Physica C* **169**, 205 (1990).

<sup>16</sup>W. W. Schmahl, A. Putnis, E. Salje, P. Freeman, A. Graeme Barber, R. Jones, K. K. Singh, J. Blunt, P. P. Edwards, J. Loram, and K. Mirza, *Philos. Mag. Lett.* **60**, 241 (1989).

<sup>17</sup>J. F. Bringley, T. M. Chen, B. A. Averill, K. M. Wong, and S. J. Poon, *Phys. Rev. B* **38**, 2432 (1988).

<sup>18</sup>R. Sonntag, D. Hohlwein, A. Hoser, W. Prandl, W. Schäfer, R. Kiemel, S. Kemmler-Sack, S. Lösch, M. Schlichenmaier, and A.W. Hewat, *Physica C* **159**, 141 (1989).

<sup>19</sup>F. Bridges, J.B. Boyce, T. Claeson, T. H. Geballe, and J. M. Tarascon, *Phys. Rev. B* **39**, 11 603 (1989).

<sup>20</sup>G. Kallias, V. Psycharis, D. Niarchos, and M. Pissas, *Physica C* **174**, 316 (1991).

<sup>21</sup>Y. Ren, W. W. Schmahl, E. Brecht, and H. Fuess, *Physica C* **199**, 414 (1992).

<sup>22</sup>T. Siegrist, L. F. Schneemeyer, J. V. Waszczak, N. P. Singh, R. L. Opila, B. Batlogg, L. W. Rupp, and D. W. Murphy, *Phys. Rev. B* **36**, 8365 (1987).

<sup>23</sup>E. Brecht, W. W. Schmahl, G. Miehe, H. Fuess, N. H. Andersen, and Th. Wolf, *Physica C* **235-240**, 471 (1994).

<sup>24</sup>E. Brecht, W. W. Schmahl, G. Miehe, M. Rodewald, H. Fuess, N. H. Andersen, J. Hanssmann, and Th. Wolf, *Physica C* **265**, 53 (1996).

<sup>25</sup>P. Zolliker, D. E. Cox, J. M. Tranquada, and G. Shirane, *Phys. Rev. B* **38**, 6575 (1988).

<sup>26</sup>P. F. Miceli, J. M. Tarascon, L. H. Greene, P. Barboux, M. Giroud, D. A. Neumann, J. J. Rhyne, L. F. Schneemeyer, and J. V. Waszczak, *Phys. Rev. B* **38**, 9209 (1988).

<sup>27</sup>P. F. Miceli, J. M. Tarascon, P. Barboux, L. H. Greene, B. G. Bagley, G. W. Hull, M. Giroud, J. J. Rhyne, and D. A. Neumann, *Phys. Rev. B* **39**, 12 375 (1989).

<sup>28</sup>I. Mirebeau, C. Bellouard, M. Hennion, G. Jehanno, V. Caignaert, A. J. Dianoux, T. E. Philipps, and K. Moorjani, *Physica C* **184**, 299 (1991).

<sup>29</sup>I. Mirebeau, C. Bellouard, M. Hennion, V. Caignaert, and E. Suard, *J. Appl. Phys.* **73**, 5689 (1993).

<sup>30</sup>I. Mirebeau, E. Suard, V. Caignaert, and F. Bouree, *Phys. Rev. B* **50**, 3230 (1994).

<sup>31</sup>J. L. Garcia-Munoz, J. Rodriguez-Carvajal, S. H. Kilcoyne, C. J. Boardman, and R. Cywinski, *J. Magn. Magn. Mater.* **104-107**, 555 (1992).

<sup>32</sup>J. L. Garcia-Munoz, R. Cywinski, S. H. Kilcoyne, and X. Obradors, *Physica C* **233**, 85 (1994).

<sup>33</sup>E. Brecht, H. Casalta, P. Schleger, N. H. Andersen, W. W.



- Schmahl, H. Fuess, and Th. Wolf, *Physica C* **235-240**, 871 (1994).
- <sup>34</sup>E. Brecht, W. W. Schmahl, H. Fuess, H. Casalta, P. Schleger, B. Lebech, N. H. Andersen, and Th. Wolf, *Phys. Rev. B* **52**, 9601 (1995).
- <sup>35</sup>H. Yasuoka, T. Shimizu, T. Imai, S. Sasaki, Y. Ueda, and K. Kosuge, ISSP Tech. Rep. 1998 (1988); *Hyperfine Interact.* **49**, 167 (1989).
- <sup>36</sup>H. Yasuoka, T. Shimizu, Y. Ueda, and K. Kosuge, *J. Phys. Soc. Jpn.* **57**, 2659 (1988).
- <sup>37</sup>Y. Yamada, K. Ishida, Y. Kitaoka, K. Asayama, H. Tagaki, H. Twabuchi, and S. Ushida, *J. Phys. Soc. Jpn.* **57**, 2633 (1988).
- <sup>38</sup>P. Mendels and H. Alloul, *Physica C* **156**, 355 (1988).
- <sup>39</sup>H. Lütgemeier, *Physica C* **153-155**, 95 (1988).
- <sup>40</sup>H. Lütgemeier and B. Rupp, *J. Phys. (France) Colloq.* **49**, C8-2147 (1988).
- <sup>41</sup>H. Lütgemeier, R. A. Brand, Ch. Sauer, B. Rupp, P. M. Meufels, and W. Zinn, *Physica C* **162-164**, 1367 (1989).
- <sup>42</sup>R. A. Brand, Ch. Sauer, H. Lütgemeier, and P. M. Meufels, *Hyperfine Interact.* **55**, 1229 (1990).
- <sup>43</sup>H. Lütgemeier, *Hyperfine Interact.* **61**, 1051 (1990).
- <sup>44</sup>H. Lütgemeier and I. Heinmaa, in *Proceedings of the of XXVI Zakopane School on Physics*, Zakopane, 1991, edited by J. Stanek and A. T. Pedziwiatr (World Scientific, Singapore, 1991), p. 264.
- <sup>45</sup>H. Lütgemeier and I. Heinmaa, in *Workshop on Phase Separation in High Temperature Superconductors*, Erice 1992, edited by K. A. Müller and G. Benedek (World Scientific, Singapore, 1992), p. 243.
- <sup>46</sup>Th. Wolf, W. Goldacker, B. Obst, G. Roth, and R. Flükiger, *J. Cryst. Growth* **96**, 1010 (1989).
- <sup>47</sup>N. H. Andersen, B. Lebech, and H. F. Poulsen, *Physica C* **172**, 31 (1990).
- <sup>48</sup>G. M. Sheldrick, computer code SHELX76, program for crystal structure determination, University of Cambridge, Cambridge, England, 1976.
- <sup>49</sup>I. Ya. Korenblit and A. Aharony, *Phys. Rev. B* **49**, 13 291 (1994).
- <sup>50</sup>N. H. Andersen and G. Uimin (unpublished).
- <sup>51</sup>W. W. Schmahl, *Ferroelectrics* **107**, 271 (1990).